
Starkindler: An Uncertainty Aware Objective for Photometric Redshift Estimation

Raahul Singh
Phaidra
rasalghul@phaidra.ai

Ashutosh Pandey
Advanced Micro Devices (AMD)
ashutosh.pandey@amd.com

Abstract

Photometric Redshift is critical for analyzing astronomical objects, but existing ML methods often overlook the aleatoric uncertainties inherent in observed data. We introduce **Starkindler**, a novel training objective that explicitly incorporates observational errors into the model’s objective function, thereby directly accounting for aleatoric uncertainty. Unlike traditional probabilistic models that focus solely on epistemic uncertainty, Starkindler provides uncertainty estimates that are regularised by aleatoric uncertainty, and is designed to be more interpretable. We train a simple convolutional neural network (CNN) using data from Sloan Digital Sky Survey (SDSS)[1] and compare against the Photometric redshift estimates provided by SDSS. We show improvements in accuracy, calibration and reduction in predicted outlier rate. We also conduct an ablation study which confirms that excluding observational errors significantly degrades model performance, underscoring the importance of accounting for aleatoric uncertainty. Our results suggest that Starkindler not only enhances predictive performance but also provides interpretable uncertainty estimates, making it a robust tool for astronomical data analysis.

1 Introduction

Redshift is the increase in the wavelength of electromagnetic radiation emitted by distant astronomical objects due to their relative motion to Earth as well as the expansion of the universe. Redshift estimation is essential for measuring galactic distances, studying their evolution, constraining cosmological models, and enabling large-scale surveys, thereby providing critical insights into the structure and dynamics of the universe[2][3]. Redshift estimation via spectroscopy (z_{spec}) is considered the gold standard due to its high accuracy and reliability in measuring the redshift of astronomical objects[4][5][6][7]. However, spectroscopy is resource-intensive, requiring significant time and effort to obtain redshift measurements for individual galaxies. This makes it impractical for large surveys that aim to study vast populations of galaxies. An alternative method, Photometric redshift estimation (z_{photo}) utilizes multi-band photometric data to estimate redshifts. While z_{photo} is more cost-effective and efficient, it is subject to higher uncertainties due to its reliance on approximations of the spectral energy distributions (SEDs) of galaxies[3]. The next generation of wide-field imaging surveys including the Rubin[8], Euclid[9] and Roman Space Telescope[10] aim to observe billions of galaxies which necessitates improvements in z_{photo} estimation techniques.

2 Related Works

Several methods use z_{spec} values as the baseline to develop models that can predict redshifts for galaxies based on their photometric data. These techniques can be broadly categorized into two main approaches: **Template Fitting** methods and **Machine Learning** methods. Template fitting methods establish the relationship between photometry and redshift by matching SEDs to a set of template SEDs. Some of the most widely used template fitting solutions are[11][12][13]. Machine learning techniques aim to directly map the relationship between photometry and redshift using supervised learning on a spectroscopic training set. Popular approaches include[14][15][16][17].

A key limitation of current template fitting and machine learning approaches is that they do not adequately account for the inherent uncertainties $zErr_{spec}$ in redshift estimation. Template-based methods use an informative prior, the underlying model of the full galaxy population to model z_{photo} . This requirement on the prior can be problematic when the template set is incomplete[18]. On the other hand, current Machine Learning based estimates of uncertainty are difficult to interpret[3], and since they do not include aleatoric uncertainty, are restricted to estimating epistemic uncertainty. This prevents these methods from being widely adopted by the scientific community.

3 Method

3.1 Methodology

Starkindler interprets the spectroscopic Redshift z_{spec} , and the redshift error ($zErr_{spec}$) (both provided by SDSS) as the mean (μ_{spec}) and standard deviation (σ_{spec}) of the ground truth target Gaussian distribution for redshift at each data point in the dataset. This modeling choice aligns with common practices in astronomy, where errors in Redshift estimates are typically treated as normally distributed [19][20][21][22], and thus includes aleatoric uncertainty in the training objective:

$$z_{spec} \sim \mathcal{N}(\mu_{spec}, \sigma_{spec}^2) \tag{1}$$

Similarly, the model takes the 5 channel photometric image X as input, and predict the mean (μ_{pred}) and standard deviation (σ_{pred}), parameterising a Gaussian distribution prediction for each image:

$$z_{pred} \sim \mathcal{N}(\mu_{pred}, \sigma_{pred}^2) \tag{2}$$

We compute the Kullback-Leibler (KL) divergence between the true and predicted Gaussian distributions, which can be computed in closed form for two Gaussians:

$$KL(z_{spec} || z_{pred}) = \log \frac{\sigma_{pred}}{\sigma_{spec}} + \frac{\sigma_{spec}^2 + (\mu_{spec} - \mu_{pred})^2}{2\sigma_{pred}^2} - \frac{1}{2} \tag{3}$$

The training objective is then the minimisation of this divergence. **To our knowledge, Starkindler is the first method to incorporate $zErr$ directly into model training, thus accounting for aleatoric uncertainty in the observed data.** To show the efficacy of the model, we train a simple CNN which has two convolutional layers with 32 channels with a kernel size of 3 each. This serves as a feature extractor which feeds two MLP heads with three hidden layer of width 1024, 512 and 32 each. We ensure non-negative predictions by clamping the mean prediction at the lower end, and using a softplus activation for the standard deviation prediction.

4 Experiments

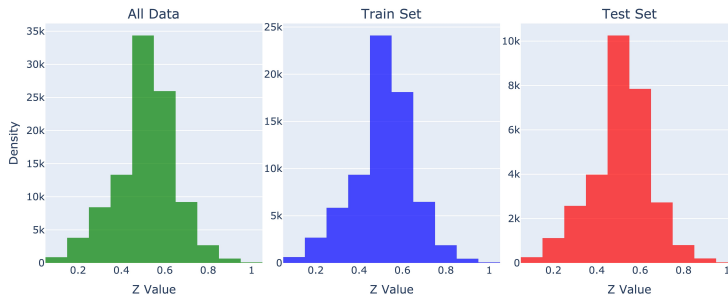


Figure 1: Test Train Split.

4.1 Dataset

We query the SDSS SkyServer archive[23] (DR17[24]) for the top 100,000 galaxies (ordered by object id) with z_{spec} values between 0.1 and 1, and get the z_{spec} , $zErr_{spec}$, z_{photo} , $zErr_{photo}$, and galactic coordinates, and download each corresponding frame. Each galaxy image extracted as a 40x40 grid centered on its coordinates (RA, Dec), with data spanning the five *UGRIZ* bands[25]. After filtering out data points with negative $zErr_{spec}$ or $zErr_{photo}$ values (which represent incorrect

data as per SDSS), we retain 99,388 images. We have provided the query to get the exact dataset from SDSS, along with code to download and process the images from SDSS servers. We perform a stratified sampling based on binned z values at 0.1 intervals to create a 70/30 train-test split giving a train and test sets with 69,571 and 29,817 images respectively, while ensuring balanced representation across the redshift range and minimizing sampling bias (Figure 1). The experiments were conducted on an M3 Pro Macbook Pro GPU, with 16GB of Unified Memory for 10 epochs.

4.2 Baseline

We compare Starkindler and the ablation model against the official SDSS photometric redshift estimates, which represent the most accurate baseline photometric redshift estimates available from SDSS[26]. As an ablation study, we also train the exact same architecture using an Negative Log Likelihood (NLL) objective wherein the only the likelihood of the observed z_{spec} is maximised, without considering the $zErr_{spec}$.

4.3 Evaluation Metrics

Redshift Prediction Accuracy: We use the Mean Squared Error (MSE), Mean Absolute Error (MAE) of mean predictions, along with scatter plots of z_{pred} vs z_{spec} as density contours with highlighted outliers, defined as instances where $|((\mu_{spec} - \mu_{pred})/(1 + \mu_{spec}))| > 0.3$, as used in [27].

Uncertainty Coverage and Calibration: Evaluated through Expected Calibration Error (ECE), Probability Integral Transform (PIT) histograms and Coverage Probability Plots.

5 Results

The results demonstrate the effectiveness of Starkindler in enhancing both accuracy and uncertainty quantification:

Method	MSE	MAE	ECE
	mean \pm std	mean \pm std	
baseline	0.0054 \pm 0.0215	0.0449 \pm 0.0582	7.46
starkindler	0.0042 \pm 0.0130	0.0441 \pm 0.0479	6.10
ablation_nll	0.0127 \pm 0.0319	0.0807 \pm 0.0787	2.55

Table 1: Performance metrics.

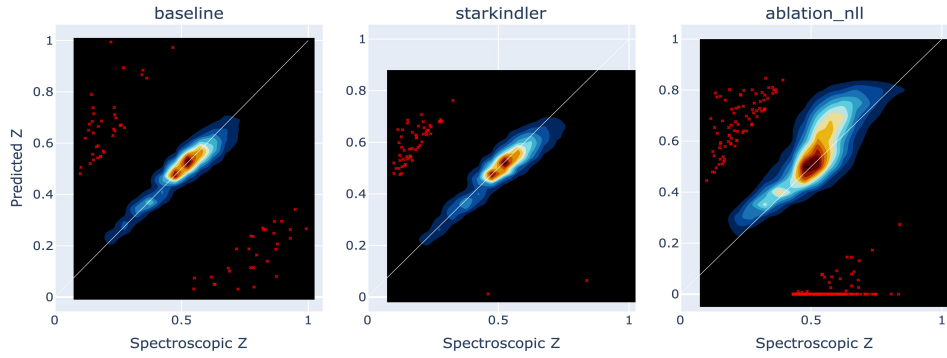
Improved Prediction Accuracy: Starkindler gets lower redshift prediction MSE and MAE errors as well as tighter error bounds as compared to the SDSS baseline (Table1), while significantly outperforming the ablation model. Starkindler gets comparable contour plots as compared to the SDSS baseline, while the ablation model shows clear bias and non uniformity in its contour plots. Starkindler also reduces the outlier prediction in higher z values in general, while particularly reducing the outliers due to under prediction of z (Figure 2a).

Improved Uncertainty Calibration: As compared to the baseline, Starkindler exhibits superior ECE values, better aligned calibration plots where alignment with the diagonal indicates better coverage (Figure 2b), and a more uniform PIT histogram (Figure 2c), indicating improved calibration over ablation_nll model. Interestingly, the ablation_nll model gets a lower ECE score but a more skewed PIT plot, indicating a degree of overestimation of uncertainties. No model gets absolutely uniform PIT histograms, indicating scope for calibration and future improvement. Starkindler shows better coverage than the baseline and the ablation model throughout.

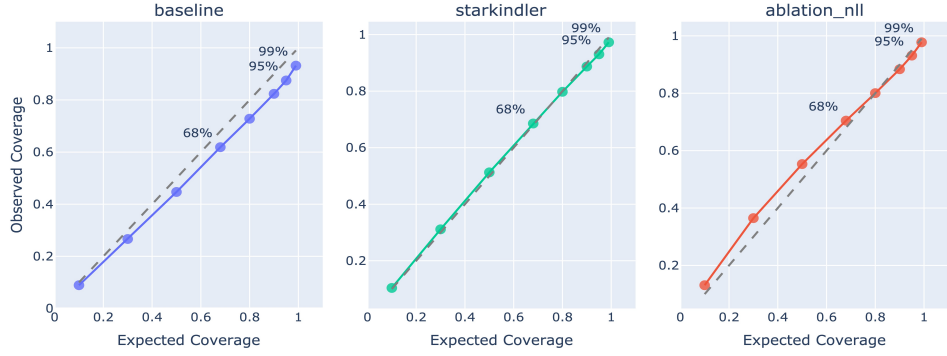
6 Discussion

Starkindler highlights the benefit of using observed error in the redshift data, $zErr_{spec}$, in the training objective of ML models.

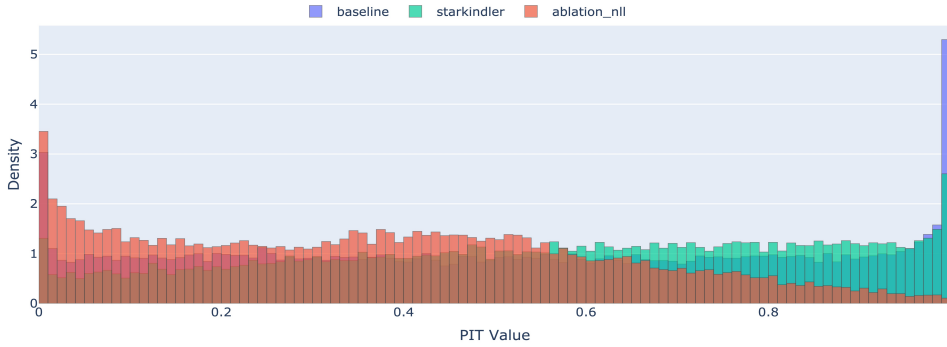
General Improvements to Prediction Accuracy and Calibration: Starkindler shows better redshift prediction accuracy with tighter error bounds and a lower outlier prediction rate as compared to the baseline. The ablation model which has the same model and training hparams and just differs in the training objective, gets poorer accuracy, worse outliers and poor calibration. While worse in predictive accuracy, the ablation model does get the lowest ECE scores which indicates the propensity



(a) Predicted Z vs Spec Z Density plot with Outliers.



(b) Probability Coverage plots.



(c) PIT Histogram

Figure 2: Comparison of Baseline, Starkindler and the Ablation models

of generic heteroskedastic models to overestimate uncertainty. This highlights the regularising effect played by inclusion of aleatoric uncertainty as provided by the Starkindler objective.

Scientific Implications: In contrast with existing probabilistic models for Redshift PDF prediction, Starkindler directly predicts the mean and standard deviation of the redshift for each photometric observation, while accounting for aleatoric uncertainty in the training data. This provides a more interpretable framework for modeling redshift errors which are critical for downstream tasks like weak lensing[28][29].

7 Future Work

Scope for improvement of existing models: Starkindler’s training objective is model agnostic and can be integrated with existing well performing models, with minimal changes to their design.

Hyper Parameter Tuning: Hyper parameter tuning may further improve model performance.

Beyond Redshift Estimation: Starkindler can also be extended beyond redshift estimation to other astrophysical measurements where inherent uncertainties estimates are available.

References

- [1] D. G. York, J. Adelman, J. E. Anderson Jr, S. F. Anderson, J. Annis, N. A. Bahcall, J. A. Bakken, R. Barkhouser, S. Bastian, E. Berman, *et al.*, “*The Sloan Digital Sky Survey: Technical summary*,” *The Astronomical Journal*, vol. 120, no. 3, p. 1579, 2000.
- [2] Lahav, O., Suto, Y., *Measuring our Universe from Galaxy Redshift Surveys*, *Living Reviews in Relativity*, 2004. <https://doi.org/10.12942/lrr-2004-8>
- [3] Newman, J. A., Gruen, D., *Photometric Redshifts for Next-Generation Surveys*, *Annual Review of Astronomy and Astrophysics*, 60, 363-414 (2022). <https://doi.org/10.1146/annurev-astro-032122-014611>
- [4] D. C. Masters, D. K. Stern, J. G. Cohen, P. L. Capak, J. D. Rhodes, F. J. Castander, and S. Paltani, “*The Complete Calibration of the Color-Redshift Relation (C3R2) Survey: Survey Overview and Data Release 1*,” *The Astrophysical Journal*, vol. 841, p. 111, June 2017.
- [5] G. Hasinger, P. Capak, M. Salvato, A. J. Barger, L. L. Cowie, A. Faisst, S. Hemmati, Y. Kakazu, J. Kartaltepe, D. Masters, B. Mobasher, H. Nayyeri, D. Sanders, N. Z. Scoville, H. Suh, C. Steinhardt, and F. Yang, “*The DEIMOS 10k spectroscopic survey catalog of the COSMOS field*,” *The Astrophysical Journal*, vol. 858, p. 77, May 2018.
- [6] M. Kriek, A. E. Shapley, N. A. Reddy, B. Siana, A. L. Coil, B. Mobasher, W. R. Freeman, L. de Groot, S. H. Price, R. Sanders, I. Shivaie, G. B. Brammer, I. G. Momcheva, R. E. Skelton, P. G. van Dokkum, K. E. Whitaker, J. Aird, M. Azadi, M. Kassis, J. S. Bullock, C. Conroy, R. Davé, D. Kere, and M. Krumholz, “*The MOSFIRE Deep Evolution Field (MOSDEF) Survey: Rest-Frame Optical Spectroscopy for ~ 1500 H-Selected Galaxies at*,” *The Astrophysical Journal Supplement Series*, vol. 218, p. 15, May 2015.
- [7] A. van der Wel, R. Bezanson, F. D’Eugenio, C. Straatman, M. Franx, J. van Houdt, M. V. Maseda, A. Gallazzi, P.-F. Wu, C. Pacifici, I. Barisic, G. B. Brammer, J. C. Munoz-Mateos, S. Vervalcke, S. Zibetti, D. Sobral, A. de Graaff, J. Calhau, Y. Kaushal, A. Muzzin, E. F. Bell, and P. G. van Dokkum, “*The Large Early Galaxy Astrophysics Census (LEGA-C) Data Release 3: 3000 High-Quality Spectra of KS-Selected Galaxies at $z > 0.6$* ,” *The Astrophysical Journal Supplement Series*, vol. 256, p. 44, Oct. 2021.
- [8] S. J. Schmidt, A. I. Malz, J. Y. H. Soo, I. A. Almosallam, M. Brescia, S. Cavuoti, J. Cohen-Tanugi, A. J. Connolly, J. DeRose, P. E. Freeman, *et al.*, “*Evaluation of probabilistic photometric redshift estimation approaches for The Rubin Observatory Legacy Survey of Space and Time (LSST)*,” *Monthly Notices of the Royal Astronomical Society*, vol. 499, no. 2, pp. 1587–1606, 2020.
- [9] M. Schirmer, K. Jahnke, G. Seidel, H. Aussel, C. Bodendorf, F. Grupp, F. Hormuth, S. Wachter, P. N. Appleton, R. Barbier, *et al.*, “*Euclid preparation-XVIII. The NISP photometric system*,” *Astronomy & Astrophysics*, vol. 662, p. A92, 2022.
- [10] T. Eifler, H. Miyatake, E. Krause, C. Heinrich, V. Miranda, C. Hirata, J. Xu, S. Hemmati, M. Simet, P. Capak, *et al.*, “*Cosmology with the Roman Space Telescope—multiprobe strategies*,” *Monthly Notices of the Royal Astronomical Society*, vol. 507, no. 2, pp. 1746–1761, 2021.
- [11] Arnouts, S., Ilbert, O., *LePHARE: Photometric Analysis for Redshift Estimate*, *Astrophysics Source Code Library*, record ascl:1108.009, 2011. <https://ui.adsabs.harvard.edu/abs/2011ascl.soft08009A>
- [12] Gabriel B. Brammer, Pieter G. van Dokkum, and Paolo Coppi, *EAZY: A Fast, Public Photometric Redshift Code*, *The Astrophysical Journal*, **686**(2), 1503 (2008), <https://dx.doi.org/10.1086/591786>,
- [13] Benítez, N. (2000). *Bayesian Photometric Redshift Estimation*. *The Astrophysical Journal*, **536**(2), 571. doi:10.1086/308947. Available at: <https://dx.doi.org/10.1086/308947>
- [14] Firth, A. E., Lahav, O., & Somerville, R. S. (2003). *Estimating photometric redshifts with artificial neural networks*. *Monthly Notices of the Royal Astronomical Society*, **339**(4), 1195-1202. doi:10.1046/j.1365-8711.2003.06271.x. Available at: <https://doi.org/10.1046/j.1365-8711.2003.06271.x>

- [15] Henghes, B., Thiyagalingam, J., Pettitt, C., Hey, T., & Lahav, O. (2022). *Deep learning methods for obtaining photometric redshift estimations from images*. Monthly Notices of the Royal Astronomical Society, **512**(2), 1696–1709. doi:10.1093/mnras/stac480. Available at: <https://doi.org/10.1093/mnras/stac480>
- [16] Schuldt, S., Suyu, S. H., Cañameras, R., Taubenberger, S., Meinhardt, T., Leal-Taixé, L., & Hsieh, B. C. (2021). *Photometric redshift estimation with a convolutional neural network: NetZ*. Astronomy & Astrophysics, **651**, A55. doi:10.1051/0004-6361/202039945. Available at: <https://www.aanda.org/articles/aa/abs/2021/07/aa39945-20/aa39945-20.html>
- [17] Z. Sun, J. S. Speagle, S. Huang, Y.-S. Ting, and Z. Cai, “*Zephyr: Stitching Heterogeneous Training Data with Normalizing Flows for Photometric Redshift Inference*,” *arXiv preprint arXiv:2310.20125*, 2023.
- [18] A. I. Malz and D. W. Hogg, “*How to obtain the redshift distribution from probabilistic redshift estimates*,” The Astrophysical Journal vol. 928, no. 2, p. 127, 2022.
- [19] R. Mandelbaum, T. Eifler, R. Hložek, T. Collett, E. Gawiser, D. Scolnic, D. Alonso, H. Awan, R. Biswas, J. Blazek, *et al.*, “*The LSST dark energy science collaboration (DESC) science requirements document*,” arXiv preprint arXiv:1809.01669, 2018.
- [20] A. D’Isanto and K. L. Polsterer, “*Photometric redshift estimation via deep learning-generalized and pre-classification-less, image based, fully probabilistic redshifts*,” Astronomy & Astrophysics, vol. 609, p. A111, 2018.
- [21] H. Oyaizu, M. Lima, C. E. Cunha, H. Lin, and J. Frieman, “*Photometric redshift error estimators*,” The Astrophysical Journal, vol. 689, no. 2, p. 709, 2008.
- [22] A. Fernández-Soto, K. M. Lanzetta, H.-W. Chen, B. Levine, and N. Yahata, “*Error analysis of the photometric redshift technique*,” Monthly Notices of the Royal Astronomical Society, vol. 330, no. 4, pp. 889–894, Mar. 2002. doi: <https://doi.org/10.1046/j.1365-8711.2002.05131.x>.
- [23] E. H. Nielsen Jr, “*The SDSS data archive server*,” Fermi National Accelerator Lab. (FNAL), Batavia, IL (United States), 2007.
- [24] None Abdurro’uf, K. Accetta, C. Aerts, V. Silva Aguirre, R. Ahumada, N. Ajgaonkar, N. Filiz Ak, S. Alam, C. Allende Prieto, A. Almeida, *et al.*, “*The seventeenth data release of the Sloan Digital Sky Surveys: Complete release of MaNGA, MaStar, and APOGEE-2 data*,” The Astrophysical Journal. Supplement Series, vol. 259, no. 2, 2022.
- [25] S. G. Sichevskij, “*Applicability of broad-band photometry for determining the properties of stars and interstellar extinction*,” Astrophysical Bulletin, vol. 73, pp. 98–107, 2018.
- [26] R. Beck, L. Dobos, T. Budavári, A. S. Szalay, and I. Csabai, “*Photometric redshifts for the SDSS Data Release 12*,” Monthly Notices of the Royal Astronomical Society, vol. 460, no. 2, pp. 1371–1381, 2016.
- [27] C. Li, Y. Zhang, C. Cui, D. Fan, Y. Zhao, X. Wu, J. Zhang, Y. Tao, J. Han, Y. Xu, *et al.*, “*Photometric redshift estimation of galaxies in the DESI Legacy Imaging Surveys*,” Monthly Notices of the Royal Astronomical Society, vol. 518, no. 1, pp. 513–525, 2023.
- [28] Samuroff, S., Troxel, M. A., Bridle, S. L., Zuntz, J., MacCrann, N., Krause, E., Eifler, T., & Kirk, D. (2016). *Simultaneous constraints on cosmology and photometric redshift bias from weak lensing and galaxy clustering*. Monthly Notices of the Royal Astronomical Society: Letters, 465(1), L20–L24. doi:10.1093/mnrasl/slw201. Available at <https://doi.org/10.1093/mnrasl/slw201>.
- [29] Hoyle, B., Gruen, D., Bernstein, G. M., Rau, M. M., De Vicente, J., Hartley, W. G., Gaztanaga, E., DeRose, J., Troxel, M. A., Davis, C., Alarcon, A., MacCrann, N., Prat, J., Sánchez, C., Sheldon, E., Wechsler, R. H., Asorey, J., Becker, M. R., Bonnett, C., Rosell, A. Carnero, Carollo, D., Kind, M. Carrasco, Castander, F. J., Cawthon, R., Chang, C., Childress, M., Davis, T. M., Drlica-Wagner, A., Gatti, M., Glazebrook, K., Gschwend, J., Hinton, S. R., Hoormann, J. K.,

Kim, A. G., King, A., Kuehn, K., Lewis, G., Lidman, C., Lin, H., Macaulay, E., Maia, M. A. G., Martini, P., Mudd, D., Möller, A., Nichol, R. C., Ogando, R. L. C., Rollins, R. P., Roodman, A., Ross, A. J., Roza, E., Rykoff, E. S., Samuroff, S., Sevilla-Noarbe, I., Sharp, R., Sommer, N. E., Tucker, B. E., Uddin, S. A., Varga, T. N., Vielzeuf, P., Yuan, F., Zhang, B., Abbott, T. M. C., Abdalla, F. B., Allam, S., Annis, J., Bechtol, K., Benoit-Lévy, A., Bertin, E., Brooks, D., Buckley-Geer, E., Burke, D. L., Busha, M. T., Capozzi, D., Carretero, J., Crocce, M., D'Andrea, C. B., da Costa, L. N., DePoy, D. L., Desai, S., Diehl, H. T., Doel, P., Eifler, T. F., Estrada, J., Evrard, A. E., Fernandez, E., Flaugher, B., Fosalba, P., Frieman, J., García-Bellido, J., Gerdes, D. W., Giannantonio, T., Goldstein, D. A., Gruendl, R. A., Gutierrez, G., Honscheid, K., James, D. J., Jarvis, M., Jeltama, T., Johnson, M. W. G., Johnson, M. D., Kirk, D., Krause, E., Kuhlmann, S., Kuropatkin, N., Lahav, O., Li, T. S., Lima, M., March, M., Marshall, J. L., Melchior, P., Menanteau, F., Miquel, R., Nord, B., O'Neill, C. R., Plazas, A. A., Romer, A. K., Sako, M., Sanchez, E., Santiago, B., Scarpine, V., Schindler, R., Schubnell, M., Smith, M., Smith, R. C., Soares-Santos, M., Sobreira, F., Suchyta, E., Swanson, M. E. C., Tarle, G., Thomas, D., Tucker, D. L., Vikram, V., Walker, A. R., Weller, J., Wester, W., Wolf, R. C., Yanny, B., & Zuntz, J. (2018). *Dark Energy Survey Year 1 Results: redshift distributions of the weak-lensing source galaxies*. Monthly Notices of the Royal Astronomical Society, 478(1), 592-610. doi:10.1093/mnras/sty957. Available at <https://doi.org/10.1093/mnras/sty957>.